processes

MDPI

Article

Calculation Model for Heat-Regulating Ring in Mine Surrounding Rock

Menglong Bian [1,*] and Lin Li [2]

[1] Mining and Coal Institute, Inner Mongolia University of Science and Technology, Baotou 014010, China
[2] Modern Service Department, Baotou Light Industry Vocational and Technical College, Baotou 014060, China; 15291961256@163.com
* Correspondence: 243519027@163.com

Abstract

The temperature of a surrounding rock mass decreases continuously due to the ventilation in its roadway, and the range of the rock mass with the temperature decreasing is called a Heat-Regulating Ring. Considering the steady-state temperature field, a steady-state heat conduction model of the Heat-Regulating Ring is established, and a formula of the radius and temperature of the Heat-Regulating Ring is obtained. It is found that the radius of the Heat-Regulating Ring is related to the thermal conductivity of the rock, the surface heat transfer coefficient of the tunnel, the radius of the ventilation tunnel, the original rock temperature, the rock wall temperature, and the air temperature. As assessed through field experiments and numerical simulation experiments, the error between the theoretical values and the simulation-derived values for the heat conduction model is very small, and the theoretical formula has a universal applicability. After long-term ventilation, the section shape and the radius of the ventilation tunnel have little effect on the Heat-Regulating Ring's radius. The wind speed increases from 1 m/s to 5 m/s, and the radius of the Heat-Regulating Ring increases from 26.9 m to 28.4 m. When the ventilation wind speed reaches a certain value, although the wind speed is still increasing, the temperature value of the Heat-Regulating Ring is basically unchanged, or the change amplitude is very small. When the wind speed is 5 m/s, after 1800 days of ventilation, the radius of the Heat-Regulating Ring along the roadway is 27.9 m to 28.4 m.

Keywords: mine thermal hazard; heat-regulating ring; steady-state heat conduction; original rock temperature; ansys fluent

check for updates

Academic Editor: Qingbang Meng

Received: 12 June 2025
Revised: 28 June 2025
Accepted: 2 July 2025
Published: 4 July 2025

Citation: Bian, M.; Li, L. Calculation Model for Heat-Regulating Ring in Mine Surrounding Rock. *Processes* **2025**, *13*, 2136. https://doi.org/10.3390/pr13072136

Copyright: © 2025 by the authors. Licensee MDPI, Basel, Switzerland. This article is an open access article distributed under the terms and conditions of the Creative Commons Attribution (CC BY) license (https://creativecommons.org/licenses/by/4.0/).

1. Introduction

With an increase in mining depth, a high-temperature and high-humidity environment forms in deep mines. This kind of thermal environment can affect the health of personnel, reduce labor productivity, weaken the strength and elastic modulus of rocks, and have a serious influence on personnel health and safe production.

There have been many case studies investigating the thermal environment in mines. J. Gonzalez-Ayala [1] developed a temperature–depth map using data measured in Avila, Spain, and designed a seasonal underground energy storage system. Jingchen Ma [2] monitored the well temperature of a geothermal field in Xiong'an New Area and found that the ranges of horizontal and vertical influence of the thermal reservoir were 262.3 m and 588.5 m, respectively. Guoqiang Yan [3] simulated the change in a nanotracer in a fractured geothermal reservoir and found that the temperature change was affected by

the geological heterogeneity. Liu Hengfeng [4] found that the distribution characteristics of the geothermal field in Kuangqu mining area are high in the north and low in the south, high in the east and low in the west, and the average heat flow value is greater than 70.1 mW/m^2. Tao Peng [5] found that the geothermal gradient in the experimental area varies from 25.7 °C/km to 54.3 °C/km, and the geothermal gradient in more than 88.31% area is greater than 30 °C/km.

A number of scholars have studied the prevention and control methods of mine heat hazards. Yujin Ran [6] proposed three heat hazard prevention strategies: ventilation system optimization, industrial waste heat utilization, and natural mine heat recovery. Amir Sedaghatkish [7] studied the heat transfer in mine tunnels, dividing the mine into three zones: a short diffusion zone, a convection zone, and a deep karst zone. Zhiying Chen [8] developed a deep mine-cooling and -strengthening geothermal system and put forward the optimization scheme of deep thermal storage and thermal recovery wellbore in Sanshandao Mine. Luwei Ding [9] proposed a mine-heating system, combining a geothermal water system with a heat pump heating system, and found that the larger the heating scale and the closer the distance, the better the economy of the system. Yu Xu [10] designed a 1:100 geothermal recovery experimental system, tested the temperature change in the rock surrounding the injection into the formation, and found that the injection time was directly proportional to the water production flow rate of the production wells and inversely proportional to the temperature of the water produced. Zhang Yongliang [11] used crushed stone, ceramsite, bamboo branches, and hollow glass microbeads to make tunnel insulation materials and found that the thermal insulation performance of the samples increased by 25~65%.

Mine heat damage comes from the surrounding rock, electromechanical equipment, hot water, and human bodies, among which the surrounding rock is the biggest source of heat damage. In the heat transfer model of mine-surrounding rock, many scholars have carried out research. Xin Chen [12] established a numerical model with which the longitudinal temperature field of a mine roadway could rapidly be calculated, and the model was in good agreement with the monitoring results for the temperature field in Dechang tunnel. In order to calculate the longitudinal heat release of a roadway, Ming Lu [13] proposed a three-dimensional implicit finite difference method considering the ventilation time and average wind speed. The difference between the calculated values and the measured values was found to be 0.94 °C. Yu Xu [14] established a fully coupled model by comprehensively considering the convective heat transfer, the unsteady heat transfer of the surrounding rock, and non-isothermal flow in a roadway and found that the deviation between the numerical model and the experimental data was less than 3%. Li Zijun [15] found that decreasing the initial airflow or increasing the ventilation speed could effectively promote latent heat release and reduce the temperature of the airflow and the surrounding rock. Xiaohan Zhou [16] adopted a convection–conduction coupling transient heat transfer model and found that the tunnel's temperature field showed periodic variation, and wind had a great influence on the tunnel's temperature field. Zhang Yuan [17] studied the heat preservation mechanism of a tunnel's insulation layer and found that the temperature gradient at the interface of different media changed abruptly. Huaitao Song [18] compared the difference between radial and axial temperature distributions in a mine and found that these two forms of temperature propagation have similar amplitude attenuation and phase delay characteristics. Wang Hao [19] established a mathematical model of the thermal insulation of the rock surrounding a deep roadway and obtained the variation law for the roadway wall's temperature with the thermal conductivity coefficient.

The heat transfer process of the surrounding rock is affected by many factors. Alessandro F. Rotta Loria [20] found that the thermal stresses in the tunnel were high, and the ther-

mal displacements were negligible through a three-dimensional thermo-hydro-mechanical finite element simulation. Yuan Zhang [21] designed an experimental device for the transient heat transfer of the tunnel-surrounding rock. It was found that with the increase in wind speed, the heat loss of surrounding rock increased, the cooling rate increased, and the speed of disturbance range expansion also accelerated. Yu Xu [22] found that the surrounding rock of roadway adjusts the underground thermal environment by absorbing or releasing heat, and the temperature distribution of the surrounding rock was "V"-shaped in winter and "W"-shape in summer. Gao Jiaan [23] studied the temperature field of the surrounding rock in an insulated roadway and found that the insulated roadway reduced the temperature difference between the original rock and the outer surface of the insulated layer.

In the process of ore mining, ventilation makes the temperature of the surrounding rock decrease continuously, and the range of temperature decrease extends to the deep part continuously. The circular body of the rock mass temperature decrease is called the Heat-Regulating Ring. Weijing Yao [24] analyzed the sensitivity of the ventilation parameters to the Heat-Regulating-Ring radius, the temperature field, and the wall temperature of the surrounding rock in Zhuji East Mine, Anhui Province. Shuai Zhu [25] found that the thermal–physical properties, the formation the thermal environment conditions, the boundary conditions, and other factors play an important role in the formation of the Heat-Regulating Ring. Yanhe Li [26] studied the influence of a composite insulation belt structure formed by injection and grouting on the tunnel heat transfer and found that the Heat-Regulating Ring in the surrounding rock gradually extended to the deep part and finally formed an elliptical cooling zone. Song Huaitao [27,28] established a dimensionless mathematical model of the heat conduction in the surrounding rock and provided a simple calculation method for the unstable heat transfer criterion of the Heat-Regulating Ring. Through the heat transfer experiment of the surrounding rock under ventilation conditions, the variation tendency of an unstable heat transfer coefficient of the Heat-Regulating Ring is obtained in the diagram [29].

The surrounding rock is the biggest source of the mine heat damage, and the Heat-Regulating Ring is the necessary channel of surrounding-rock heat dissipation. At present, the concept of the Heat-Regulating Ring is vague, and the heat transfer mechanism of the Heat-Regulating Ring is not clear. It is of great significance for the prevention and control of heat damage to study the heat conduction in the Heat-Regulating Ring. In practical production, the thermal boundary parameters and the ventilation parameters of a roadway surface are known or measurable, but the radius variation in the Heat-Regulating Ring and the distribution law of the temperature field are difficult to grasp, and it is difficult to establish an effective correlation between the Heat-Regulating Ring and roadway thermal boundary parameters and ventilation parameters, which makes for a lack of deep understanding of the interaction and influence between roadway ventilation and the surrounding rock mass.

Considering that the Heat-Regulating Ring will eventually reach a relatively stable state, the heat conduction problem of the Heat-Regulating Ring is solved via the idea of steady-state heat conduction. The heat conduction model of the Heat-Regulating Ring is simplified and regarded as a huge cylinder. The heat conduction coefficient of the rock and tunnel surface are regarded as fixed values. The heat conduction differential equation is established and solved. Through field experiments and numerical simulation experiments, the theoretical model error is very small, and it has universal applicability.

2. Steady-State Heat Conduction Model of the Heat-Regulating Ring

With the increase in the ventilation time in the tunnel, the radius of the Heat-Regulating Ring increases gradually, during which the thermal conductivity of rock in Heat-Regulating Ring and the surface heat transfer coefficient of the tunnel wall will change correspondingly [30]. When the surrounding rock is homogeneous and isotropic, the thermal conductivity and the surface heat transfer coefficient of the rock are only functions of temperature, and the variation amplitude of the two coefficients is small in this range, so they can be considered as fixed values.

There is no numerical standard for the Heat-Regulating Ring at present; in order to analyze the problem conveniently, the following assumptions are put forward: the cooling range in which the temperature of the surrounding rock decreases by 0.1% and exceeds the original rock temperature is considered as the Heat-Regulating Ring; when the temperature decreases below 0.1 °C one day, the Heat-Regulating Ring can be considered to reach a stable state. Assuming that the Heat-Regulating Ring reaches a steady state after a long-enough ventilation time, the state can be regarded as infinitely close to the steady-state heat transfer under the condition of constant ventilation parameters, and the heat transfer problem of the Heat-Regulating Ring can be analyzed using the steady-state heat transfer model.

The heat conduction relationship for the cross section of the Heat-Regulating Ring is analyzed, as shown in Figure 1. The dark part in the figure is the Heat-Regulating Ring, and the white part is the tunnel. The rock mass at different depths has different original rock temperatures. Considering the concept of a geothermal temperature increase rate, the original rock temperatures at different depths can be considered as linearly increasing with depth [31,32]. In the figure, the original rock temperatures of the Heat-Regulating Ring at point A above the roadway, point B at the same level, and point C below the roadway are $t_0 - \Delta t$, t_0, and $t_0 + \Delta t$, respectively. The two points A and C are in the same vertical direction, and the roadway rock wall temperature is t_w.

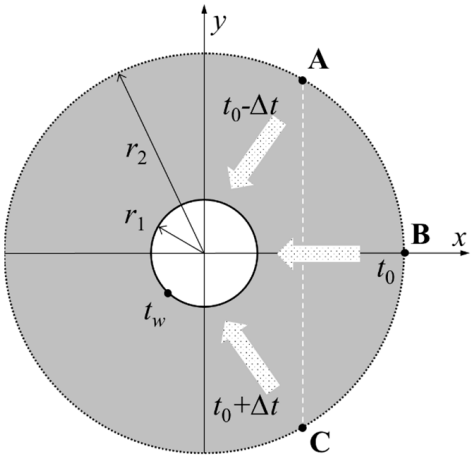


Figure 1. A schematic diagram of the heat conduction at the cross-section of the Heat-Regulating Ring.

According to Fourier's law, the heat flux is expressed as Equation (1):

$$q = -\lambda \frac{dt}{dx} \tag{1}$$

where q is the heat flux density, W/m; λ is thermal conductivity of the rock, W/(m·K); dt/dx is the temperature change rate, where the negative sign indicates that the heat transfer direction is opposite to the temperature increase direction.

The heat flux density generated by the heat conduction from the three points in Figure 1 to the tunnel wall is shown in the following three equations:

$$q_A = \lambda \frac{(t_0 - \Delta t) - t_w}{r_2 - r_1} = \lambda \frac{t_0 - \Delta t - t_w}{r_2 - r_1}$$
$$q_B = \lambda \frac{t_0 - t_w}{r_2 - r_1}$$
$$q_A = \lambda \frac{(t_0 + \Delta t) - t_w}{r_2 - r_1} = \lambda \frac{t_0 + \Delta t - t_w}{r_2 - r_1}$$

By analyzing the above equations, Equation (2) is obtained.

$$q_A + q_C = 2q_B \tag{2}$$

The upper and lower parts in Figure 1 are symmetrical in structure, and the average heat flux density of the outer boundary of the Heat-Regulating Ring is equal to the heat flux density generated in the middle direction of the Heat-Regulating Ring (i.e., the heat flux generated from point B to the tunnel wall direction). The heat conduction model of the Heat-Regulating Ring can be simplified to the heat conduction model with the original rock temperature of the outer boundary being a constant value (temperature of point B).

The Heat-Regulating Ring is assumed to be a large cylinder with a ventilation tunnel inside and thermal boundary condition of constant temperature of raw rock outside. The ventilation tunnel is a circular tunnel, the tunnel radius is r_1, the Heat-Regulating-Ring radius is r_2, the original rock temperature is t_0, the rock wall temperature is t_w, and the tunnel air temperature is t_f, as shown in Figure 2.

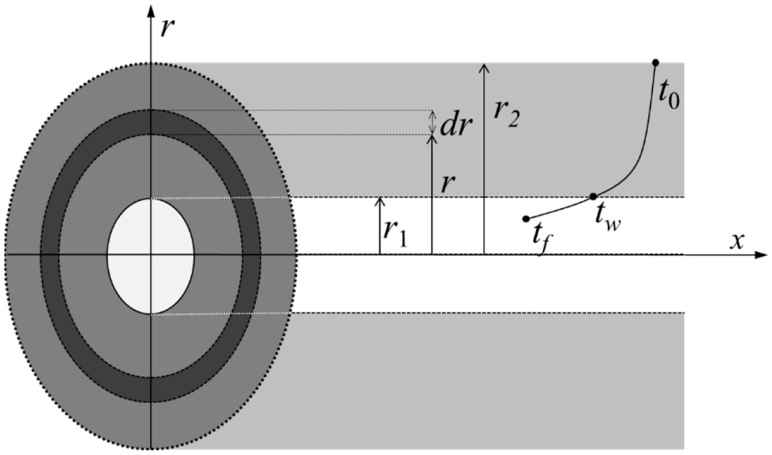


Figure 2. A schematic diagram of heat conduction in the Heat-Regulating Ring.

After a sufficient ventilation time, the heat conduction of the cross-section of the Heat-Regulating Ring is a one-dimensional heat conduction problem. The heat conduction differential equation and the corresponding boundary conditions are as follows:

$$\begin{gathered} \frac{d}{dr}\left(r\frac{dt}{dr}\right) = 0 \\ r = r_1,\ t = t_w \\ r = r_2,\ t = t_0 \end{gathered} \tag{3}$$

The solution of Equation (3) by continuous integration is shown in Equation (4):

$$t = c_1 lnr + c_2 \tag{4}$$

where the c_1 and c_2 depend on boundary conditions. Substituting boundary conditions into the equation, the temperature distribution at radius r is obtained as shown in Equation (5).

$$t = t_w + \frac{t_0 - t_w}{ln(r_2/r_1)} ln(r/r_1) \tag{5}$$

Derivating the above equation, the following equation is obtained:

$$\frac{dt}{dr} = \frac{1}{r} \frac{t_0 - t_w}{ln(r_2/r_1)}$$

Substituting the above equation into Fourier's law translates into Equation (6).

$$q = \frac{\lambda}{r} \frac{t_0 - t_w}{ln(r_2/r_1)} \tag{6}$$

From Equation (6), it can be seen that the heat flux density at different radii is inversely proportional to the radius. The heat transfer form in the Heat-Regulating Ring is heat conduction, and the heat transfer forms in the roadway rock wall are heat convection and heat radiation. Without considering the action of water, O_2 and N_2 in the air, as diatomic gases, basically do not participate in heat radiation, and only the influence of heat convection should be considered in the heat dissipation of the mine-surrounding rock.

The heat flux density of the convective heat transfer from rock walls can be expressed as Equation (7):

$$q_d = h\left(t_w - t_f\right) \tag{7}$$

where h is surface heat transfer coefficient, $W/(m^2 \cdot K)$.

In the case of the steady-state heat conduction, the heat flux density at the rock wall is equal, i.e., $q = q_d$. Combining Equations (6) and (7), the following equation is obtained (note that in Equation (6), $r = r_1$):

$$\frac{\lambda}{r} \frac{t_0 - t_w}{ln(r_2/r_1)} = h\left(t_w - t_f\right)$$

Further simplification yields Equation (8).

$$r_2 = r_1 exp\left[\frac{\lambda(t_0 - t_w)}{r_1 h\left(t_w - t_f\right)}\right] \tag{8}$$

Equation (8) is the formula for calculating the Heat-Regulating-Ring radius. It can be seen from Equation (8) that the Heat-Regulating-Ring radius is related to the thermal conductivity λ of the rock, the surface heat transfer coefficient h of the tunnel, the radius of the ventilation tunnel r_1, the original rock temperature t_0, the rock wall temperature t_w, and the air temperature t_f. As shown in Figure 2, in the x direction, i.e., the ventilation direction of the tunnel, the air temperature and the rock wall temperature rise continuously due to the heat transfer temperature, and the radius r_2 of the Heat-Regulating Ring may also change according to Equation (8).

Due to the limitation of experimental conditions, Equation (8) is verified with field experiments and numerical simulation experiments. In the numerical simulation experiment, the Heat-Regulating-Ring radius and temperature variation are tested under different tunnel radius and ventilation parameters.

3. Validation of Experimental Data

In order to eliminate the interference of mine cars, the high-temperature and -humidity area without mine cars was selected as the test site. The test data of the original rock temperature at −662 m in Xiadian Gold Mine was selected to verify the results. The field experiment has obtained the research permission of Xiadian Gold Mine.

The original rock-temperature-measuring instrument is a single-point digital thermometer, the instrument model is CX-WDJ 200 LCD (Shanghai Innovation Instrument Co., Ltd., Shanghai, China), and the measuring range is −50~+200 °C; the measurement error is 0.1 °C, as shown in Figure 3a. Since the radius of the Heat-Regulating Ring is generally not more than 30 m, the rock-drilling depth is set as 30 m, and the temperature of the measuring point is taken as the original rock temperature, as shown in Figure 3b. Under normal ventilation conditions, after drilling for 48 h, the thermometer is bound with the steel bar, and the steel bar goes deep into the hole for the temperature measurement. When measuring, measure point by point from outside to inside, arrange a measuring point every 2.5 m, record the data after the reading of the measuring instrument is stable, and collect the air flow temperature and wind speed data in the roadway near the measuring point.

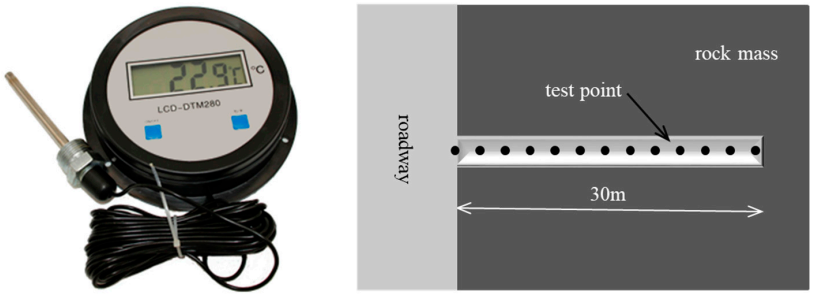


Figure 3. Rock-temperature-measuring instrument (**a**) and measuring point arrangement (**b**).

During the experiment, a temperature and humidity recorder (The instrument model is RC-4, Jiangsu Jingchuang Electric Co., Ltd., Xuzhou, China) was used to record the temperature and relative humidity changes in the environment, with a temperature range of −30~60 °C and the relative humidity range of 0~99%, the measurement error is 0.1 °C, as shown in Figure 4a. Use an anemometer (The instrument model is AZ9651, Taiwan Hengxin Instrument Co., Ltd., Taiwan, China) to record the wind speed and air pressure, with the wind speed ranging from 0 to 45 m/s; the measurement error is 0.1 m/s, as shown in Figure 4b. Before the experiment, the test instruments were calibrated. During the experiment, the instruments were placed in a stable environment strictly according to the requirements of instrument use.

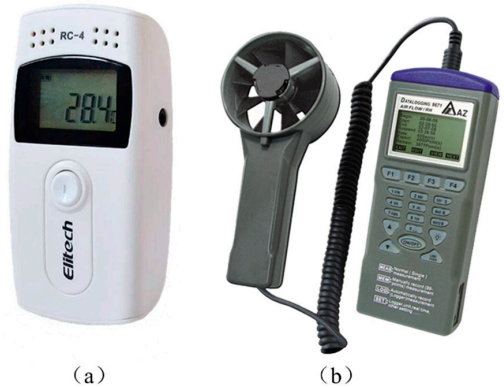


Figure 4. The temperature and humidity recorder (**a**) and the anemometer (**b**).

The arch tunnel has a sectional area of 23.2 m^2, the thermal conductivity λ= 3 W/(m·K), the original rock temperature t_0 = 30.8 °C, the rock wall temperature t_w = 30.4 °C, the air temperature t_f = 29.9 °C, the convective heat transfer coefficient h = 0.6 w/(m^2·K), and r_2 = 11.84 m, calculated by substituting Equation (8). The measured original rock temperature and the depth of the measuring point are shown in Figure 5.

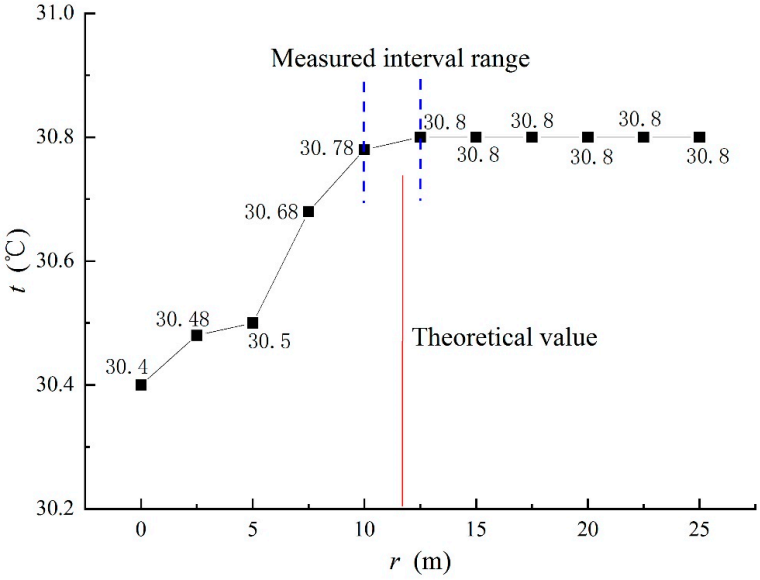


Figure 5. Measured temperature of original rock and theoretical radius of Heat-Regulating Ring.

It can be seen from Figure 5 that the rock mass temperature increases correspondingly with the increase in the depth of the measuring point. After the depth of the measuring point reaches 12.5 m, the rock mass temperature remains unchanged at 30.8 °C. It can be seen that the original rock temperature for this section of roadway is 30.8 °C. According to the depth of the measuring point and the temperature change in the original rock, it can be known that the radius of the Heat-Regulating Ring is between 10 m and 12.5 m, and the theoretical value calculated according to formula is 11.84 m in the range of the measured interval. The theoretical value is consistent with the experimental value. Equation (8) can be used to calculate or predict the radius of the Heat-Regulating Ring.

4. Numerical Simulation Experiments

4.1. Model and Parameter Setting of Heat-Regulating Ring

ANSYS 2023 R1 is selected as the numerical simulation platform (The software provided by USTB, Beijing, China). Simulating experiments are carried out on the heat conduction of the Heat-Regulating Ring under various tunnel radii and ventilation parameters. In the model, the radius of the rock mass is 50 m, the radius of the roadway is 0.5~4 m, and the length of the roadway is 500 m. As shown in Figure 6, the numerical model diagram of the roadway radius is 2 m.

The "mesh" software is used to generate meshes. Tetrahedron mesh division method is mainly adopted, with a mesh number of 431220 and a node number of 457846. The mesh independence analysis is as follows: For a model with a radius of 2 m, take three points of the exit section (500, −0.5, 0) (500, 0, 0) (500, 0.5, 0). When the total numbers of grids are 431220, 474164, 597220, 714820, and 1467336, respectively, under the condition of a wind speed of 5 m/s and a ventilation time of 1800 days, the temperature value of three points changes very little, and the difference is less than 0.1 °C, which indicates that the number of grids has little influence on the calculation results. It can be considered that the

grid number of 431220 has reached the grid independence, so the grid number of 431220 is selected as the calculation grid.

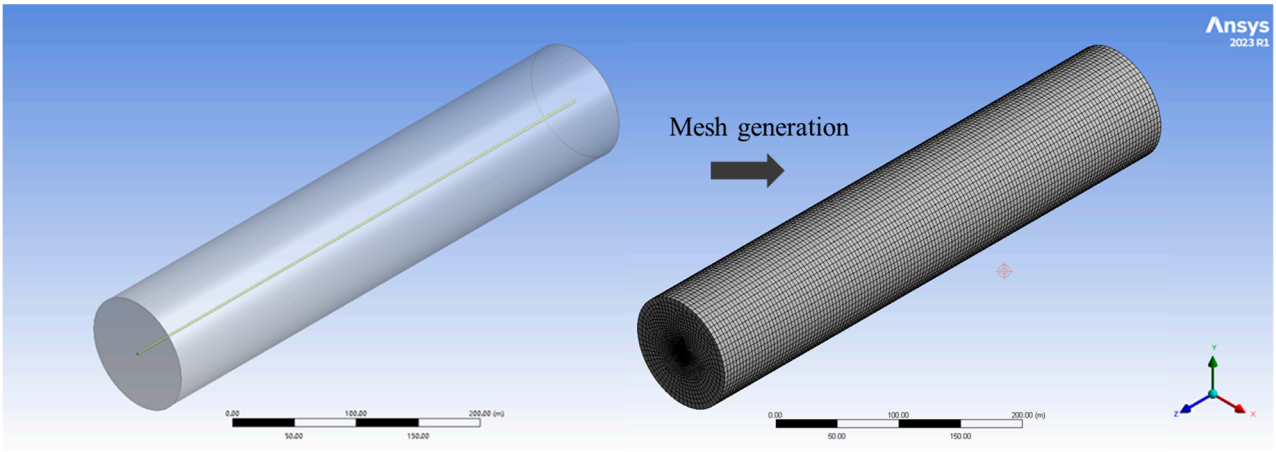


Figure 6. Model diagram of Heat-Regulating Ring.

Parameter settings are shown in Table 1.

Table 1. Parameters setting in Fluent.

Parameter Names	Setting Information
Solver	Pressure-based solver
Time	Unsteady state
Energy equation	Open
Model	Realizable k-ε model
Turbulence intensity	2.75–3.4%
Hydraulic diameter	1–8 m
Inlet velocity	1–5 m/s
Inlet temperature	20 °C
Entry boundary type	Velocity entry
Exit boundary type	Free export
Wall boundary	50 °C
Texture	Custom rock material properties
Calculation method	SIMPLE

4.2. Influences of Tunnel Section on Heat-Regulating-Ring Radius

In the numerical simulation experiments, the tunnel sections are set as circle, rectangle, and arch, respectively, and the influence of different section types on the radius of the Heat-Regulating Ring is tested. As shown in Figure 7, the value of R2 in the figure is the average value at 100 m, 250 m, and 400 m from the entrance in the tunnel model.

The total ventilation time is 1800 days, the Heat-Regulating-Ring radii of the circular section, rectangular section, and arch section are 7 m, 8.5 m, and 8.3 m, respectively, when the ventilation time is 30 days; the Heat-Regulating-Ring radii of the circular section, rectangular section, and arch section are 16.9 m, 18.2 m, and 17.6 m, respectively, when the ventilation time is 300 days. When the ventilation time is 600 days, the three values are 21.6 m, 22.2 m, and 21.9 m, respectively, and when the ventilation time is 900 days, the three values are 25.1 m, 25.1 m, and 25.3 m, respectively. At this time, the influence of the section change on the Heat-Regulating-Ring radius is very small and can be ignored.

As can be seen from the data change in Figure 7, if the ventilation time is long enough, the tunnel section shape has no effect on the radius of the Heat-Regulating Ring.

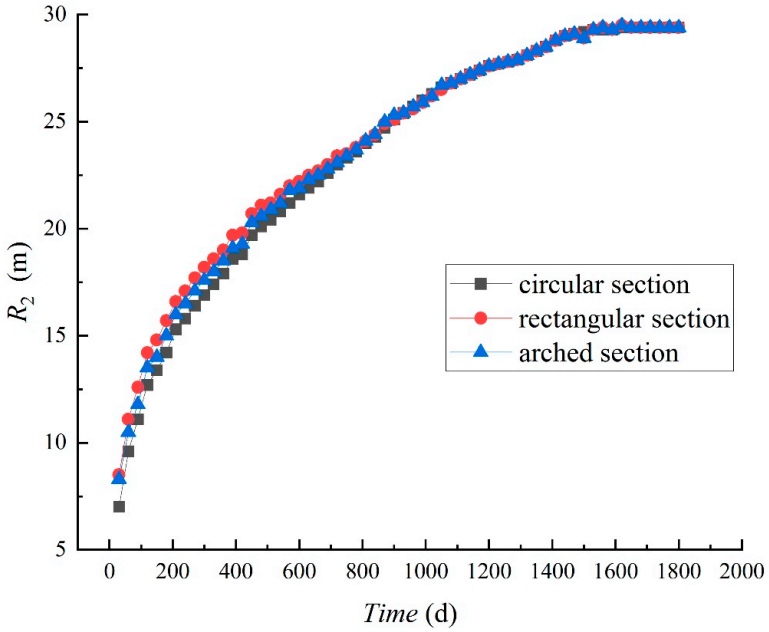


Figure 7. Heat-Regulating-Ring radius under different tunnel section conditions.

4.3. Effects of Ventilation Time on Heat-Regulating-Ring Radius

The wind speed of 5 m/s, the radius of Heat-Regulating Ring r_1 of 2 m, and the change in Heat-Regulating-Ring radius in the process of ventilation for 1800 days are selected for the explanation. Figure 8a–d show the temperature field distribution of the Heat-Regulating Ring at 30 days, 180 days, 360 days, and 1800 days, respectively. It can be seen intuitively from Figure 8 that the radius of the Heat-Regulating Ring changes slowly with the ventilation time, and this radius change can only be reflected after a sufficient ventilation time.

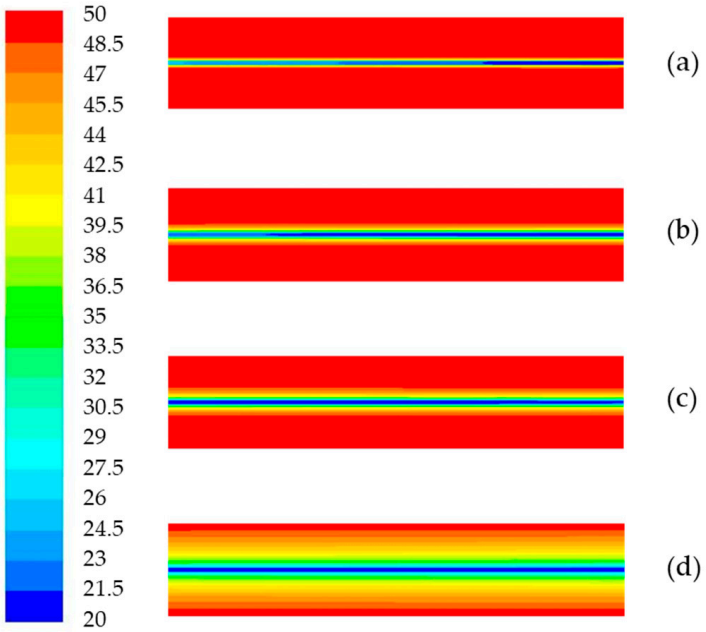


Figure 8. Heat-Regulating-Ring radius at different ventilation time: (**a**) 30 days, (**b**) 180 days, (**c**) 360 days, and (**d**) 1800 days.

After 1800 days (nearly 5 years) of ventilation, the radius of the Heat-Regulating Ring increases below 0.1 m every 30 days, and the daily variation amplitude is less than 0.0034 m. The Heat-Regulating Ring is relatively stable. At this time, the Heat-Regulating Ring can be

considered as relatively stable, and the heat conduction problem of the Heat-Regulating Ring can be solved by the steady-state heat conduction. After 1800 days of ventilation, the radius of the Heat-Regulating Ring is 27.9~28.4 m along the distance of the 500 m long roadway. It can be seen that the radius of Heat-Regulating Ring after a long-enough ventilation varies little along the roadway trend, which can be ignored in engineering calculation.

4.4. Effects of Wind Speed on Heat-Regulating-Ring Radius

Change the ventilation wind speed, adopt the same tunnel model (r_1 = 2 m), and collate the experimental data to form Figure 9 after the same simulation time of 1800 days.

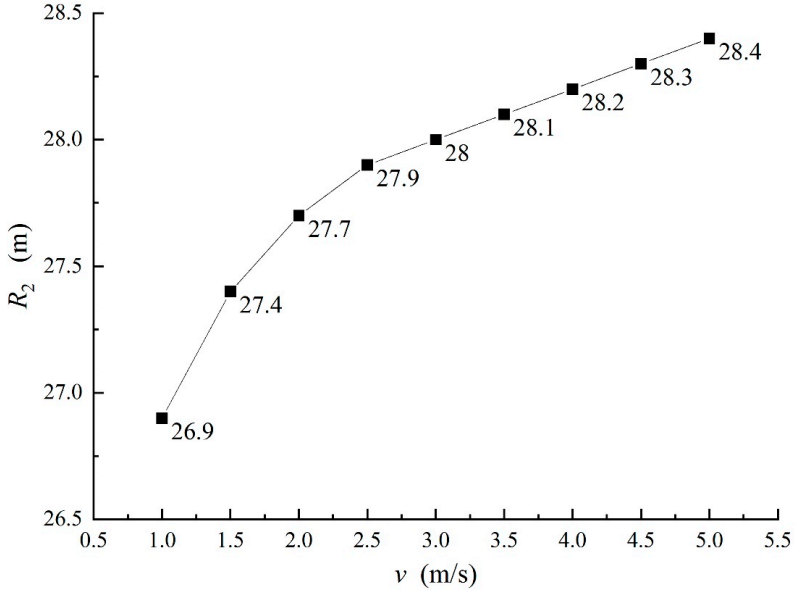


Figure 9. Data of Heat-Regulating-Ring radius at different velocities.

As can be seen from Figure 9, the wind speed increases from 1 m/s to 5 m/s, and the radius of the Heat-Regulating Ring increases from 26.9 m to 28.4 m. When the wind speed reaches 2.5 m/s, the radius of the Heat-Regulating Ring increases by only 0.1 m. In a certain ventilation time, the larger the wind speed, the larger the radius of the Heat-Regulating Ring, and the radius increase gradually weakened.

According to Equation (8), the theoretical value of the Heat-Regulating-Ring radius under different wind speeds is verified to be consistent with the simulated experimental value. Under different wind speeds, the thermal conductivity λ = 3 W/(m·K), tunnel radius r_1 = 2 m, raw rock temperature t_0 = 50 °C, air temperature t_f = 20 °C, and t_w are determined according to simulation experimental data.

The surface heat transfer coefficient h is calculated with reference to Equation (9) [30]:

$$h = \frac{\lambda}{D} N_u = 0.023 \frac{\lambda}{D} Re^{0.8} Pr^{0.4} \tag{9}$$

where λ is the thermal conductivity of the fluid, W/(m·K); D is the characteristic length, m; Nu is the Nusselt number; Re is the Reynolds number; Pr is the Planck number.

The surface heat transfer coefficient h reflects the influence of different wind speeds. Theoretical values are calculated according to Equation (8), and numerical simulation experimental values are shown in Table 2. In the table, the r_2 refers to the theoretical value calculated according to Equation (8), the R_2 refers to the experimental value of numerical simulation, and δ is the relative error, $\delta = (R_2 - r_2)/R_2$.

Table 2. The theoretical and experimental values of the Heat-Regulating-Ring radius under different wind speeds.

v/m·s^{-1}	h/W·m^{-2}·K^{-1}	t_w/°C	R_2/m	r_2/m	δ
1	2.75	25.2	26.9	26.9	0
1.5	3.8	23.9	27.4	28	−2%
2	4.79	23.2	27.7	27.6	0.4%
2.5	5.73	22.7	27.9	28.3	−1.4%
3	6.62	22.4	28	27	3.6%
3.5	7.49	22.1	28.1	28.6	−1.8%
4	8.34	21.9	28.2	28.6	−1.4%
4.5	9.16	21.7	28.3	30.5	−7.8%
5	9.97	21.6	28.4	28.9	−1.8%

Comparing r_2 with R_2, it is found that the difference between r_2 and R_2 is less than 1 °C, and the relative error is between −7.8% and 3.6%. The radius of the Heat-Regulating Ring calculated by Equation (8) basically accords with the experimental results.

4.5. Influence of Tunnel Radius on Heat-Regulating-Ring Radius

When the wind speed is 5 m/s and the ventilation time is 1800 days, the theoretical value and experimental values of the Heat-Regulating-Ring radius under different tunnel radii are shown in Figure 10.

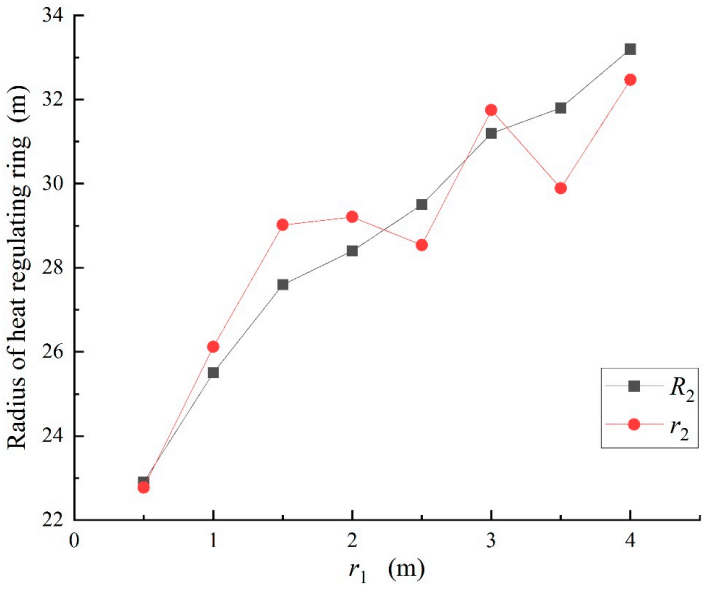


Figure 10. Tunnel radius and Heat-Regulating-Ring radius.

When the tunnel radius r_1 is 0.5 m, the theoretical calculation value r_2 of the Heat-Regulating-Ring radius is 22.99 m, and the numerical simulation experimental value R_2 is 22.9 m. When the tunnel radius is 1 m, the r_2 and R_2 are 26.12 m and 25.5 m, respectively; when the tunnel radius is 3.5 m, the r_2 and R_2 are 29.9 m and 31.8 m, respectively; the difference between them reaches 1.9 m, and the difference reaches the maximum; when the tunnel radius is 4 m, the r_2 and R_2 are 32.47 m and 33.2 m, respectively, and the difference between them reaches 0.73 m. It can be seen from the data in the figure that when the radius of the roadway increases, the Heat-Regulating-Ring radius will increase accordingly, but if the radius of the roadway changes slightly, the influence on the Heat-Regulating-Ring radius is very small, which can be ignored in engineering calculations. Comparing the theoretical value r_2 with the experimental value R_2, the difference between

them is basically within the acceptable range. Under the condition of different tunnel radii, the Heat-Regulating-Ring radius calculated by Formula (8) basically accords with the experimental results.

4.6. Calculation of Heat-Regulating Ring Internal Temperatures

Equation (5) reflects the relationship between the rock mass temperature and other parameters at a certain depth in the Heat-Regulating Ring, which can be used to calculate rock mass temperature at a certain point. The following is verified according to the numerical simulation results, where $r_1 < r < r_2$: After the ventilation of 5 m/s for 1800 days, the theoretical value t_l and the experimental value t_s at different r positions in the Heat-Regulating Ring are verified, where t_0 = 50 °C, t_w = 21.6 °C, r_1 = 2 m, and r_2 = 28.4 m.

At the rock mass 5 m, 10 m, 15 m, 20 m, and 25 m away from the tunnel center, the t_l values are 31.4 °C, 38.8 °C, 43.2 °C, 46.2 °C, and 48.6 °C, respectively; the t_s values are 31.8 °C, 39.5 °C, 43.5 °C, 46.1 °C, and 47.8 °C, respectively; the maximum difference between t_l and t_s is 0.8 °C, and the difference between t_l and t_s is very small. Analyzing the data in Figure 11, the theoretical temperature value and the experimental temperature value at different r positions are very close to each other, and the internal temperature calculations of the Heat-Regulating Ring using Formula (5) are very close to the numerical simulation's experimental values.

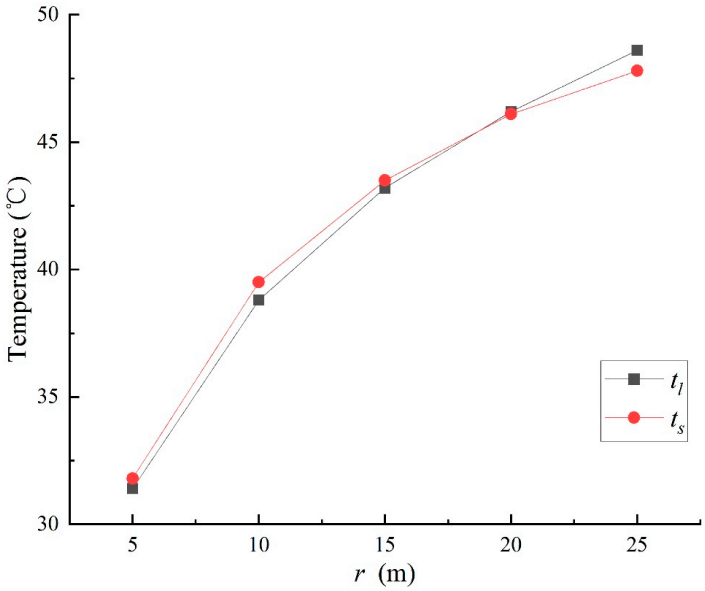


Figure 11. Temperature distribution at different distances from the tunnel center in the longitudinal section of the Heat-Regulating Ring.

The values calculated by Equations (5) and (8) give results closer to the experimental values. The thermal conductivity λ of the rock, the surface heat transfer coefficient h of the tunnel, the radius r_1 of the ventilation tunnel, the original rock temperature t_0, the rock wall temperature t_w, and the air temperature t_f in the two equations can be measured or obtained by consulting geological and hydrological data. When using the two equations, the values of λ, h, t_0, t_w, and t_f must be accurate to ensure that the results are as close to the actual state of the Heat-Regulating Ring as possible. Equations (5) and (8) are derived from the fundamental theory of heat transfer and are therefore of general applicability.

5. Conclusions

Considering the Heat-Regulating Ring with a sufficient ventilation time as a steady-state heat conduction model, the temperature and radius of the Heat-Regulating Ring are

proposed. Equations (5) and (8) are verified with measured data and numerical simulation experiments. The theoretical results are close to the actual heat conduction of the Heat-Regulating Ring, and the formula has theoretical and practical value.

With the increase in the ventilation wind speed, the Heat-Regulating-Ring radius will increase accordingly. If the ventilation time is long enough, the Heat-Regulating-Ring radius will be slightly affected by the ventilation wind speed; with the increase in the ventilation wind speed, the internal temperature of the Heat-Regulating Ring will decrease correspondingly, and the decreasing amplitude will gradually decrease with the increase in the Heat-Regulating-Ring depth; when the wind speed reaches a certain value, although the wind speed is still increasing, the temperature value of the Heat-Regulating Ring is basically unchanged or the changing amplitude is very small.

The Heat-Regulating-Ring radius, which has experienced sufficient ventilation for a long time varies very little along the roadway trend, and this difference can be ignored in engineering calculations. The wind speed increases from 1 m/s to 5 m/s, and the radius of the Heat-Regulating Ring increases from 26.9 m to 28.4 m.

If the ventilation time is long enough, the section shape of the roadway has no effect on the Heat-Regulating-Ring radius. When the wind speed is 5 m/s, after 1800 days of ventilation, the radius of the heat regulation circle along the roadway is 27.9 m to 28.4 m.

When the radius of the ventilation tunnel increases, the Heat-Regulating-Ring radius will increase correspondingly, but if the radius of the ventilation tunnel changes slightly, the influence on the Heat-Regulating-Ring radius is very small, and this influence can also be ignored in engineering calculations.

Author Contributions: Conceptualization, M.B. and L.L.; methodology, M.B.; software, M.B.; validation, L.L.; investigation, M.B. and L.L.; data curation, M.B. and L.L.; writing—original draft preparation, M.B. and L.L.; writing—review and editing, M.B. All authors have read and agreed to the published version of the manuscript.

Funding: This research was funded by the Fundamental Research Funds for Inner Mongolia University of Science & Technology, grant number 2024QNJS100; the Inner Mongolia Autonomous Region Natural Science Foundation, grant number 2023QN05020; the Inner Mongolia University of Science and Technology Scientific Research Start-up Foundation, grant number 0303052203.

Data Availability Statement: The original contributions presented in this study are included in the article. Further inquiries can be directed to the corresponding author.

Conflicts of Interest: The authors declare no conflicts of interest.

References

1. Gonzalez-Ayala, J.; Blázquez, C.S.; Lagüela, S.; Nieto, I.M. Assesment for optimal underground seasonal thermal energy storage. *Energy Convers. Manag.* **2024**, *308*, 118394. [CrossRef]
2. Ma, J.; Liu, Z.; Wang, Z.; Guo, S.; Liu, X.; Huang, Y. The influence of different mining modes on the heat extraction performance of hydrothermal geothermal energy. *Energies* **2024**, *17*, 1922. [CrossRef]
3. Yan, G.; Andersen, P.Ø.; Qiao, Y.; Hatzignatiou, D.G.; Nitschke, F.; Spitzmüller, L.; Kohl, T. Numerical modeling of temperature-reporting nanoparticle tracer for fractured geothermal reservoir characterization. *Geoenergy Sci. Eng.* **2024**, *237*, 212787. [CrossRef]
4. Liu, H.; Zhang, J.; Rodriguez-Dono, A.; Zhou, N.; Wang, Y.; Sun, Q.; Li, B. Utilization of mine waste heat in phase change rechargeable battery. *Appl. Therm. Eng.* **2023**, *233*, 121136. [CrossRef]
5. Peng, T.; Liu, K.; Chen, Y.; Wang, F.; Li, B.; Xin, L. Main controlling factors and formation mode of geothermal anomaly in eastern chenghe mining area of Weibei Coalfield. *Geofluids* **2022**, *2022*, 3209790. [CrossRef]
6. Ran, Y.; Peng, J.; Tian, X.; Luo, D.; Zhao, J.; Pei, P. Technologies for heat hazard governance and thermal energy recovery in deep mines. *Energies* **2024**, *17*, 1369. [CrossRef]
7. Sedaghatkish, A.; Pastore, C.; Doumenc, F.; Jeannin, P.; Luetscher, M. Modeling heat transfer for assessing the convection length in ventilated caves. *J. Geophys. Res. Earth Surf.* **2024**, *129*, e2024JF007646. [CrossRef]

8. Chen, Z.; Huang, L.; Li, X.; Chen, J.; Liu, Z. Comprehensive heat extraction performance and fractured reservoir cooling effect analysis of a novel mine enhanced geothermal system. *Appl. Therm. Eng.* **2024**, *245*, 122790. [CrossRef]
9. Ding, L.; Zhang, Z.; Li, B.; Qi, S.; Liu, H.; Liu, S. Feasibility investigation of geothermal energy heating system in mining area: Application of mine cooling and aquifer thermal energy exploitation technique. *Energies* **2024**, *17*, 1168. [CrossRef]
10. Xu, Y.; Li, Z.; Tao, M.; Jalilinasrabady, S.; Wang, J.; Li, G.; Zhong, K. An investigation into the effect of water injection parameters on synergetic mining of geothermal energy in mines. *J. Clean. Prod.* **2023**, *382*, 135256. [CrossRef]
11. Zhang, Y.; Yin, S.; Qu, M.; Liu, Y.; Zhu, Z.; Zhou, Y.; Zhu, Q.; Xing, Y. Feasibility of natural bamboo branches aggregate applied to the thermal insulation layer of rock walls in roadways. *Constr. Build. Mater.* **2024**, *435*, 136870. [CrossRef]
12. Chen, X.; Zhou, X.; Zhong, Z.; Liang, N.; Wang, Y.; Zhang, X. Study on temperature field and influencing factors of the high geothermal tunnel with extra-long one-end construction ventilation. *Int. J. Therm. Sci.* **2023**, *191*, 108322. [CrossRef]
13. Lu, M.; Yu, L.; Wang, M.; Sun, B.; Zhou, Z.; Tang, Y. A new approach in calculation of heat release during high geothermal tunnels construction considering ventilation time effect. *Int. J. Therm. Sci.* **2023**, *194*, 108589. [CrossRef]
14. Xu, Y.; Li, Z.; Liu, H.; Jia, M.; Wang, Q.; Zhang, M.; Xu, Y. Modeling of the dynamic behaviors of heat transfer during the construction of roadway using moving mesh. *Case Stud. Therm. Eng.* **2021**, *26*, 100958. [CrossRef]
15. Li, Z.; Xu, Y.; Li, R.; Jia, M.; Wang, Q.; Chen, Y.; Cai, R.; Han, Z. Impact of the water evaporation on the heat and moisture transfer in a high-temperature underground roadway. *Case Stud. Therm. Eng.* **2021**, *28*, 101551. [CrossRef]
16. Zhou, X.; Ren, X.; Ye, X.; Tao, L.; Zeng, Y.; Liu, X. Temperature field and anti-freezing system for cold-region tunnels through rock with high geotemperatures. *Tunn. Undergr. Space Technol.* **2021**, *111*, 103843. [CrossRef]
17. Zhang, Y.; Wan, Z.; Ma, Z.; Gu, B.; Ma, Y. Heat transfer analysis of surrounding rocks with thermal insulation layer in high geothermal roadway. *Therm. Sci.* **2019**, *23*, 777–790. [CrossRef]
18. Song, H.; Qin, Y.; Wu, J.; Wang, G.; Li, S.; Niu, C.; Wu, Z.; de Monte, F. Study on the radial and axial temperature fields of coal roadway under seasonal fluctuation boundary. *Math. Probl. Eng.* **2019**, *2019*, 2120618. [CrossRef]
19. Wang, H.; Zhou, Q.; Garg, A. Finite element analysis of surrounding rock with a thermal insulation layer in a deep mine. *Math. Probl. Eng.* **2020**, *2020*, 5021853. [CrossRef]
20. Loria, A.F.R.; Di Donna, A.; Zhang, M. Stresses and deformations induced by geothermal operations of energy tunnels. *Tunn. Undergr. Space Technol.* **2022**, *124*, 104438. [CrossRef]
21. Zhang, Y.; Wan, Z.; Gu, B.; Zhou, C. An experimental investigation of transient heat transfer in surrounding rock mass of high geothermal roadway. *Therm. Sci.* **2016**, *20*, 2149–2158. [CrossRef]
22. Xu, Y.; Li, Z.; Li, G.; Jalilinasrabady, S.; Zhai, X.; Chen, Y.; Wang, B. A thermal environment prediction method for a mine ventilation roadway based on a numerical method: A case study. *Case Stud. Therm. Eng.* **2023**, *42*, 102733. [CrossRef]
23. Gao, J.; Li, S.; Wu, F.; Ma, L. Heat transfer model and thermal insulation characteristics of surrounding rock of thermal insulation roadway in a high-temperature mine. *Sustainability* **2023**, *15*, 12555. [CrossRef]
24. Yao, W.; Pang, J.; Ma, Q.; Lyimo, H. Influence and sensitivity analysis of thermal parameters on temperature field distribution of active thermal insulated roadway in high temperature mine. *Int. J. Coal Sci. Technol.* **2021**, *8*, 47–63. [CrossRef]
25. Zhu, S.; Cheng, J.; Song, W.; Borowski, M.; Zhang, Y.; Yu, B.; Wang, Y.; Qi, C.; Tukkaraja, P.; Hua, G.; et al. Using seasonal temperature difference in underground surrounding rocks to cooling ventilation airflow: A conceptual model and simulation study. *Energy Sci. Eng.* **2020**, *8*, 3457–3475. [CrossRef]
26. Li, Y.; Wan, Z.; Yu, Z.; Shi, P.; Zhang, B.; Zhang, Y. Numerical simulation research on thermal insulation performance of composite heat insulation zone structure in hydrothermal high temperature mine. *Sci. Rep.* **2024**, *14*, 14096. [CrossRef]
27. Song, H.; Li, J.; Yu, Y.; Chen, Q. Research on the influence of subway tunnel depth on heat storage characteristics of the surrounding soil mass. *Appl. Sci.* **2023**, *13*, 9534. [CrossRef]
28. Song, H.; Chen, Q. Dimensionless analysis of soil temperature field of shallow subway tunnel. *Energy Build.* **2022**, *259*, 111900. [CrossRef]
29. Tu, Q.; Yu, C.; Li, Z.; Tao, X.; Miao, L. Computer simulation study on heat transfer of surrounding rock in mine roadway of coal mine enterprises. *Therm. Sci.* **2020**, *24*, 3049–3058. [CrossRef]
30. Bian, M.; Li, L. Application of human thermal comfort evaluation method in deep stope of Xiadian Gold Mine. *Discov. Appl. Sci.* **2025**, *7*, 419. [CrossRef]
31. Xiao, D.; Hu, Y.; Wang, Y.; Deng, H.; Zhang, J.; Tang, B.; Xi, J.; Tang, S.; Li, G. Wellbore cooling and heat energy utilization method for deep shale gas horizontal well drilling. *Appl. Therm. Eng.* **2022**, *213*, 118684. [CrossRef]
32. Xiao, D.; Liu, M.; Li, L.; Cai, X.; Qin, S.; Gao, R.; Liu, J.; Liu, X.; Tang, H.; Li, G. Model for economic evaluation of closed-loop geothermal systems based on net present value. *Appl. Therm. Eng.* **2023**, *231*, 121008. [CrossRef]

Disclaimer/Publisher's Note: The statements, opinions and data contained in all publications are solely those of the individual author(s) and contributor(s) and not of MDPI and/or the editor(s). MDPI and/or the editor(s) disclaim responsibility for any injury to people or property resulting from any ideas, methods, instructions or products referred to in the content.